

STRUCTURAL AND BIOCHEMICAL CHANGES IN LOBLOLLY PINE (*PINUS TAEDA* L.) SEEDS DURING GERMINATION AND EARLY-SEEDLING GROWTH. I. STORAGE PROTEIN RESERVES

SANDRA L. STONE AND DAVID J. GIFFORD¹

Department of Biological Sciences, University of Alberta, Edmonton, Alberta T6G 2E9, Canada

Quantitative and qualitative changes in the storage proteins of loblolly pine (*Pinus taeda* L.) seeds were followed during germination and early-seedling growth and were correlated with light-microscopic observations. In both the megagametophyte and the embryo, the cells of tissues from fully stratified seeds appeared very similar to the cells of tissues from mature desiccated seeds. A change in the appearance of protein vacuoles, resulting from the hydrolysis of storage proteins, occurred in the seedling prior to the completion of germination (denoted by radicle emergence from the seed coat) and continued during early-seedling growth. Within the seedling, storage proteins were mobilized more rapidly in the root pole, including the hypocotyl and radicle, than in the shoot pole, including the cotyledonary whorl, and shoot apex or epicotyl. In both parts of the seedling, protein hydrolysis was first observed in the procambial and epidermal tissue. In contrast to the seedling, changes in the appearance of protein vacuoles were not evident in the megagametophyte until after germination was completed. Changes in protein vacuoles in the megagametophyte occurred in two directional waves, relative to corrosion cavity proximity.

Introduction

The mature desiccated seed of loblolly pine consists of three integument layers, the remnant of the nucellus, the megagametophyte, and the embryo. The two outer integuments form the hard seed coat, and the innermost integument is a thin papery layer that is separate from the hard seed coat and covers the entire megagametophyte. Between the innermost integument and the megagametophyte is the remnant of the nucellus, the nucellar cap, which is found at the micropylar end of the seed. The diploid embryo resides in a space within the haploid megagametophyte termed the *corrosion cavity* (Singh and Johri 1972; Hoff 1987).

The primary storage reserves of many conifer seeds are lipids and proteins that are contained in lipid bodies and protein vacuoles (protein bodies), respectively (Gori 1979; Krasowski and Owens 1993). Although these reserves are present in both the embryo and the megagametophyte, the majority are stored in the megagametophyte (Ching 1966; Sasaki and Kozlowski 1969; Gifford 1988; Kovac and Kregar 1989). During germination and early-seedling growth, storage protein reserves are degraded to amino acids (Durzan and Chalupa 1968; Salmia 1981; Lammer and Gifford 1989; King and Gifford 1997), and storage lipids are converted to soluble carbohydrates (Ching 1966). The soluble carbohydrates (Murphy and Hammer 1988) and amino acids (Lammer and Gifford 1989; King and Gifford 1997) are transported to the seedling. In the seedling, they provide the building blocks and energy necessary for growth and the development of photosynthetic autonomy (Sasaki and Kozlowski 1969; Durzan et al. 1971; Murphy and Hammer 1994). The mechanism of this transport has yet to be determined.

Quantitative changes in seed storage reserves during

and after germination have been described in several conifer species, as have changes in cell-free activity of enzymes believed to be involved in reserve metabolism during this period (Hammer and Murphy 1994; Misra 1994; Mullen and Gifford 1995; King and Gifford 1997). Structural changes related to the breakdown of seed storage reserves have also been described; for the most part, these other studies focus on subcellular changes occurring in specific tissues. For example, in megagametophyte cells, a decrease in protein vacuole and lipid body number occurred primarily after germination was completed (Simola 1974b, 1976; Gori 1979). Correlated with this depletion of storage organelle contents in the megagametophyte cells was an increase in the number of microbodies, which were likely glyoxysomes. In contrast, in seedling cotyledons (Durzan et al. 1971; Simola 1974a, 1974b; De Carli et al. 1987), hypocotyls (De Carli et al. 1987), and radicles/roots (Simola 1974b, 1976), the decrease in protein vacuole and lipid body numbers was initiated during germination and progressed into early-seedling growth. These changes were accompanied by an in-

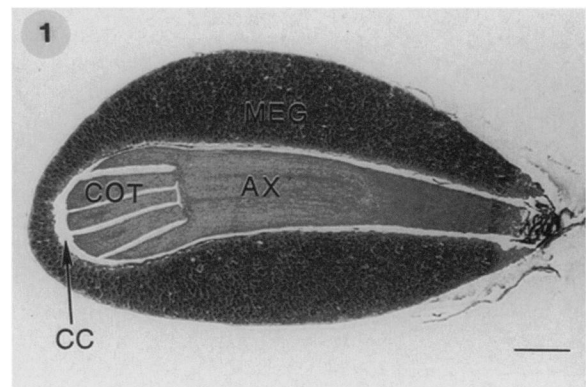
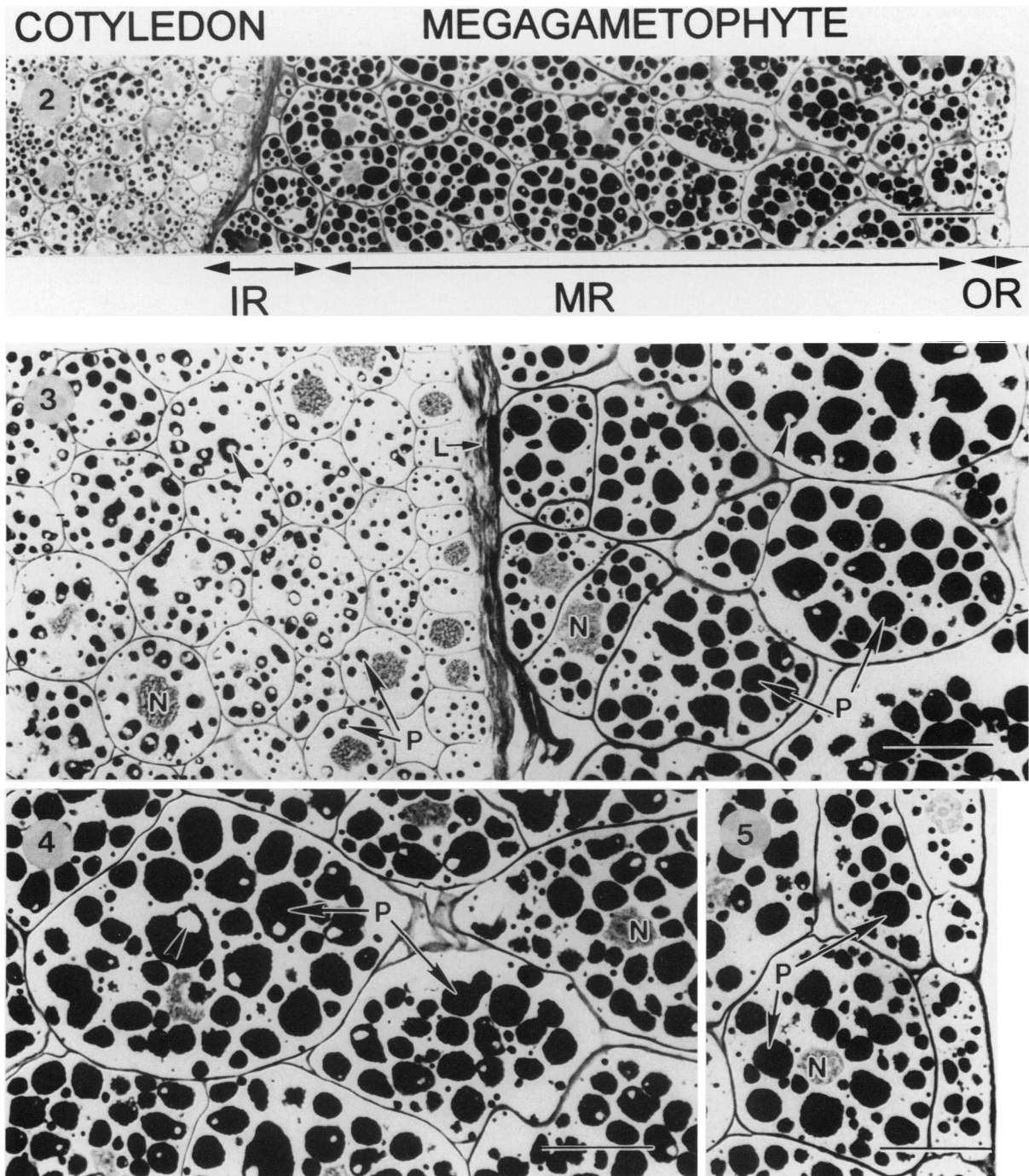


Fig. 1 Light micrograph of a longitudinal section through a paraffin-embedded mature seed with integuments removed. Megagametophyte (MEG), cotyledons (COT), embryonic axis (AX), and corrosion cavity (CC) are shown. Bar = 700 μ m.

¹Author for correspondence and reprints; fax 403-492-9234; E-mail david.gifford@ualberta.ca.

Manuscript received September 1997; revised manuscript received May 1997.



Figs. 2-5 Light micrographs of transverse sections through a plastic-embedded 35 DAI, stratified seed showing three different regions of the megagametophyte. Protein vacuoles (*P*), globoids (arrowheads), and nucleus (*N*) are shown. Fig. 2, Overview of the megagametophyte in relation to the cotyledons. Bidirectional arrows indicate the three regions examined. Inner region (*IR*), middle region (*MR*), and outer region (*OR*) are shown. Bar = 60 μm . Fig. 3, Enlarged view of the megagametophyte inner region consisting of one to three layers of cells next to the carbohydrate-positive layer (*L*). A portion of the middle region is also shown. A cotyledon is closely appressed to the carbohydrate-positive layer, so the corrosion cavity that is normally present between the cotyledon and the carbohydrate-positive layer is difficult to see. Bar = 30 μm . Fig. 4, Enlarged view of the center of the middle region. Cells are large and contain numerous protein vacuoles. Bar = 30 μm . Fig. 5, Enlarged view of the outer region, consisting of a single layer of epidermal-type cells, next to the middle region. Bar = 30 μm .

crease in numbers of organelles such as endoplasmic reticulum, dictyosomes, mitochondria, and plastids.

Some studies have compared the relative timing of structural events in the different tissues of conifer

seeds during germination and early-seedling growth. For example, the initiation and progression of subcellular organelle changes in the megagametophyte and different areas of the seedling have been compared in

Picea abies (Simola 1974a, 1976), *Picea excelsa* (De Carli et al. 1987), and *Pinus sylvestris* (Simola 1974b). In *Araucaria araucana*, amyloplast disappearance was compared among the radicle, cotyledons, and megagametophyte (Cardemil and Reiner 1982) and between the tissues of the megagametophyte and cotyledonary tube of *A. bidwillii* (Burrows and Stockey 1994). In only a few studies have structural changes been correlated with biochemical changes that occur during germination and early-seedling growth. In cotyledonary cells of *Pinus banksiana*, a decrease in the level of total buffer-soluble protein was correlated with the occurrence of protein body cavities (Durzan et al. 1971). Changes in the number of amyloplasts in the cells of the megagametophyte, radicle, and cotyledons of *A. araucana* seeds were correlated with megagametophyte, embryo and seedling amylase activity, soluble sugar levels, and starch levels (Cardemil and Reiner 1982). The cotyledon region in *P. excelsa* seedlings that had emerged from the megagametophyte contained highly vacuolated cells and differentiated chloroplasts, while the cotyledon region that still remained inside the megagametophyte contained less vacuolated cells with less differentiated chloroplasts. Associated with the more highly differentiated cotyledon region was a higher level of O₂ release and a higher level of chlorophyll a and b content. (De Carli et al. 1987). Using both structural and biochemical approaches, we have investigated the temporal and spatial patterns of storage protein breakdown in loblolly pine (*Pinus taeda* L.) megagametophytes and embryos during germination and early-seedling growth.

Material and methods

SEED, GERMINATION, AND EARLY-SEEDLING GROWTH

Loblolly pine seeds, kindly provided by Westvaco (Summerville, S.C.) were collected in the fall of 1992 from an open-pollinated first-generation tree (clone 11-9). All seeds were surface sterilized prior to stratification, stratified in darkness for 35 d at 2°C (DAI₂) to break dormancy (Groome et al. 1991), and then allowed to germinate at 30°C (DAI₃₀) with continuous fluorescent light (19 μmol μm⁻² s⁻¹). Following germination (4 DAI₃₀), as indicated by radicle emergence through the seed coat, the seeds were maintained at 30°C

(DAI₃₀) with continuous fluorescent light (19 μmol m⁻² s⁻¹) for up to 8 d. Early-seedling growth was defined as the period after radicle emergence but before the seedling shed the megagametophyte. Seeds were staged according to the method of Mullen et al. (1996).

Seeds at maturity, at 35 DAI₂ and at different DAI₃₀, were separated into megagametophytes, embryo or seedling shoot poles (including the cotyledonary whorl and shoot apex or epicotyl), and embryo or seedling root poles (including the hypocotyl and the radicle). In addition, whole embryos from mature seeds were collected. Mature seeds were imbibed for 1 h prior to dissection. We use the term *embryo* to describe the sporophyte from both mature desiccated seeds and fully stratified seeds. The term *seedling* is used to describe the sporophyte from germinating seeds and seeds after germination.

LIGHT MICROSCOPY AND HISTOCHEMISTRY

For whole mature desiccated seeds, the hard seed coat and thin papery layer were removed, leaving the nucellar cap still attached to the megagametophyte (fig. 1). Thin longitudinal sections through the nucellar cap, megagametophyte, and embryo were fixed with formalin-acetic acid-alcohol, dehydrated, and embedded in paraffin. After paraffin blocks were softened in Gifford's solution 1 (Gifford 1950) for 7 d, 10-μm sections were cut and stained with methyl violet 2B and erythrosin (Jensen 1962).

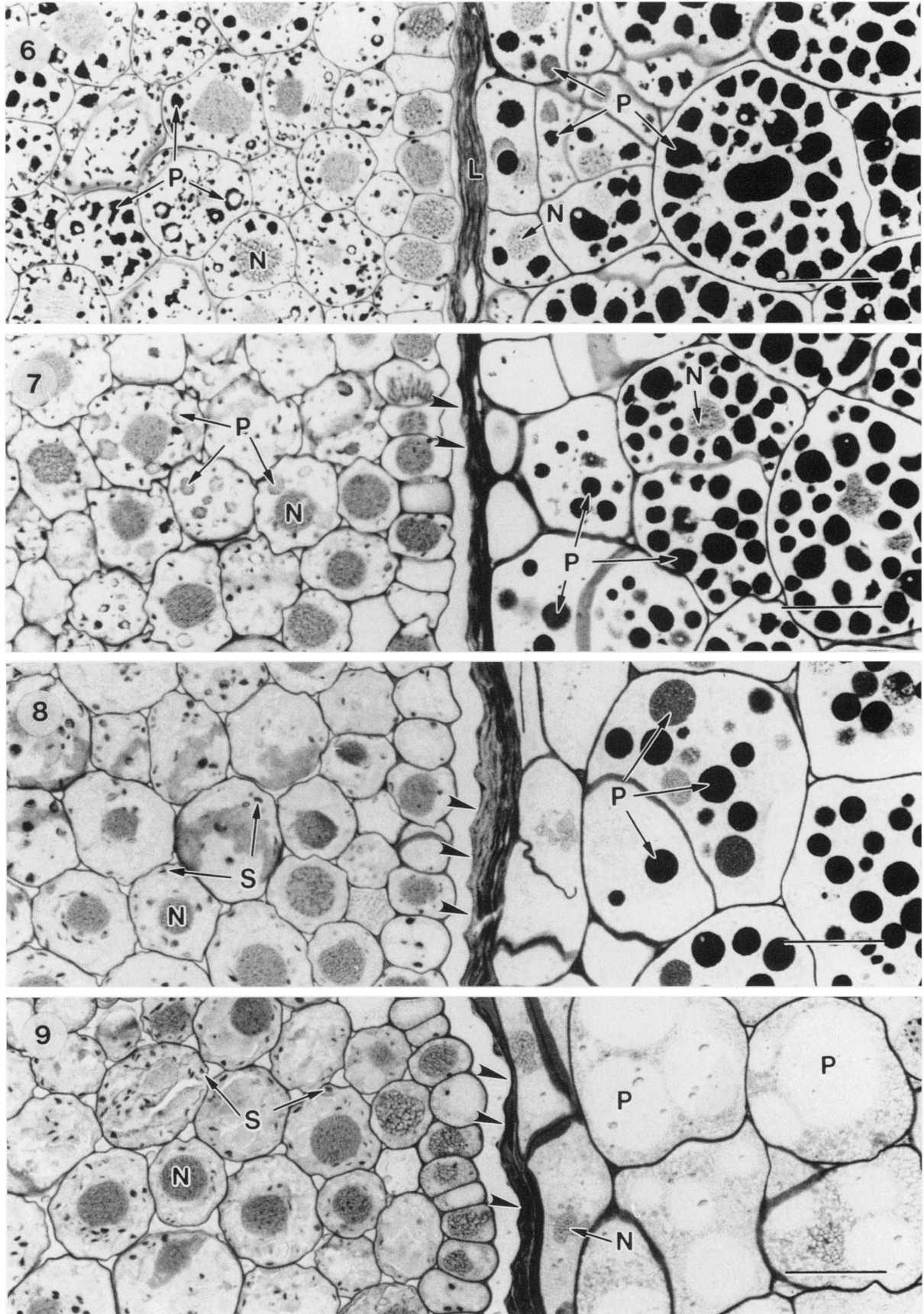
For developmental studies, the hard seed coat, thin papery layer, and nucellar cap were removed from stratified (35 DAI₂) and 2–12 DAI₃₀ seeds. Thin slices through the seed, transverse to the cotyledons or to the hypocotyl, were cut and fixed by freeze substitution (Jensen 1962). The seed tissues were plunged into 12% methyl-cyclohexane in 2-methylbutane cooled by liquid nitrogen and were then transferred to a vial containing 100% methanol previously cooled in a dry ice/acetone bath. Sample vials were stored at -70°C for 6 d, and during this time the methanol was changed three times. After 6 d, the vials were slowly brought to room temperature over a period of 3 h. Methanol was replaced with propylene oxide, and specimens were embedded in Spurr's resin (Spurr 1969). Specimens were sectioned at 1.5 μm, stained with periodic acid-Schiff's reaction for carbohydrates (Jensen 1962), and counter stained with Aniline Blue Black for proteins (O'Brien and McCully 1981). Because of their brittle nature, mature desiccated seeds were surface sterilized and imbibed for 24 h at 2°C before integument removal and freeze substitution.

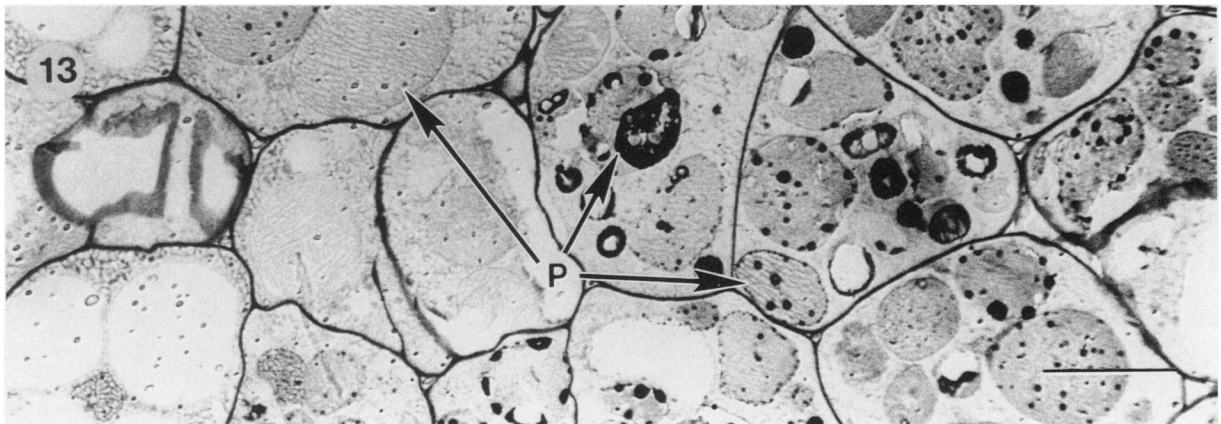
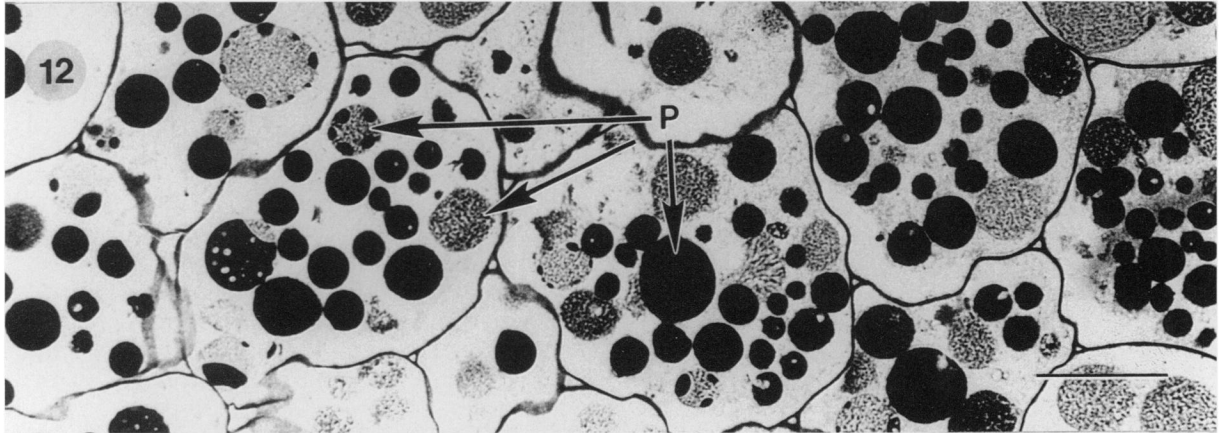
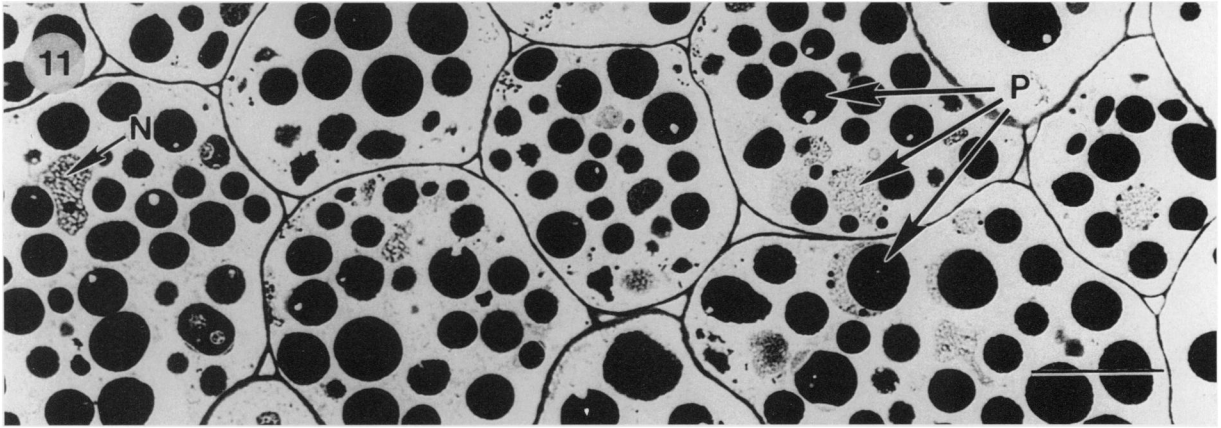
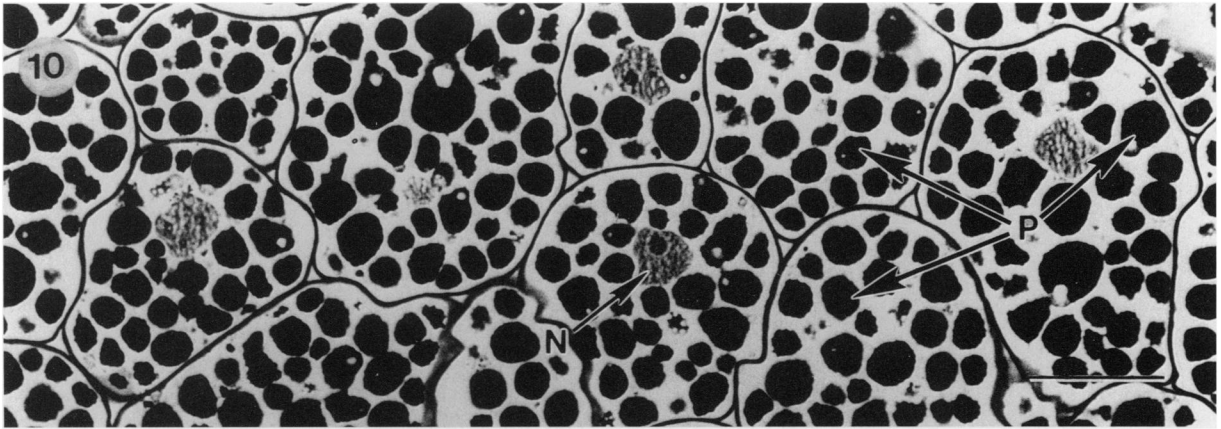
PROTEIN EXTRACTION AND QUANTIFICATION

Prior to analysis, megagametophytes and embryo or seedling parts were frozen in liquid nitrogen and stored at -70°C.

Figs. 6–9 Light micrographs of transverse sections through seeds in the area of a cotyledon (left of the figs.) and megagametophyte during imbibition at 30°C. Cotyledon epidermal cell imprints (arrowheads) are visible in carbohydrate-positive layer (*L*). Nucleus (*N*) and protein vacuole (*P*) are shown. Bars = 30 μm. Fig. 6, 5 DAI₃₀. Megagametophyte inner-region cells are beginning to swell. Protein vacuoles in this region are undergoing protein depletion. Protein vacuoles in the developing mesophyll of the cotyledon are also undergoing protein depletion. Fig. 7, 6 DAI₃₀. Inner megagametophyte cells are swelling further. Protein vacuoles in the cotyledon are depleted of most of their protein. Fig. 8, 10 DAI₃₀. Very few protein vacuoles are left in the inner megagametophyte region. Starch grains (*S*) are visible in cotyledon cells. Fig. 9, 12 DAI₃₀. Inner-region cells contain protein vacuoles depleted of protein.

Figs. 10–13 Light micrographs of transverse sections through the center of the megagametophyte middle region during imbibition at 30°C. Micrographs are oriented so that the inner region is to the left and the outer layer is to the right. Nucleus (*N*) and protein vacuole (*P*) are shown. Bars = 30 μm. Fig. 10, 6 DAI₃₀. Cells contain numerous protein vacuoles. Fig. 11, 9 DAI₃₀. Protein vacuoles are larger and more variable in appearance than in the six DAI₃₀ cells. Fig. 12, 11 DAI₃₀. Protein vacuoles are fewer in number and variable in appearance. Fig. 13, 12 DAI₃₀. Most of the protein vacuoles have been depleted of protein.





To determine the protein content of mature seed tissues, 10 megagametophytes were ground in a total of 5 mL of 0.05 M sodium phosphate buffer pH 7.5 and centrifuged at 20,000 *g* at 4°C for 20 min, and the supernatants were assayed for buffer-soluble proteins. The pellet was then re-extracted in a total of 7 mL of Laemmli buffer (Laemmli 1970) with 15 min of boiling and centrifuged at 20,000 *g* at room temperature for 20 min, and the supernatants were assayed for buffer-insoluble proteins. A similar procedure was used to determine the protein content of 20 mature whole embryos, with 3 mL 0.05 M sodium phosphate buffer pH 7.5 and 3 mL Laemmli buffer. For measurement of the protein content of seed parts collected from maturity through to 12 DAI₃₀, we used the method of Groome et al. (1991). Protein was quantified by the method of Lowry et al. (1951), using BSA as standard.

ELECTROPHORESIS

SDS-PAGE and sample preparation were carried out as described by Laemmli (1970) using a mini-PROTEAN II electrophoresis system (Bio-Rad), with a 0.75 mm 12% slab gel at 200 V. Following electrophoresis, proteins were visualized with Coomassie blue R (Burk et al. 1983). Molecular mass markers included phosphorylase b, 97.4 kD; BSA, 66.2 kD; ovalbumin, 45 kD; carbonic anhydrase, 31 kD; soybean trypsin inhibitor, 21.5 kD; and lysozyme, 14.4 kD (Bio-Rad).

Results

STRUCTURAL CHANGES IN THE MEGAGAMETOPHYTE AND IN THE EMBRYO OR SEEDLING

At the light-microscopic level, tissues of mature desiccated and fully stratified seeds were very similar in appearance. For descriptive purposes, the megagametophyte was divided into three regions: an inner, a middle, and an outer region (fig. 2). The inner region, approximate to the corrosion cavity, varied from one to three cells in thickness (fig. 3). Cells in this region often contained incomplete cell walls, were sometimes polynucleate, and appeared flattened or squashed in transverse section. Projecting into the corrosion cavity from the inner region was a carbohydrate-positive layer of variable thickness (fig. 3). In the mature desiccated seed, this layer appeared to be composed of several flaky sheets, whereas in the stratified seed, it was more mucilaginous and malleable. In some areas of the stratified seed, the hydrated carbohydrate layer filled much of the corrosion cavity space between the embryo and megagametophyte. The middle region contained cells that were larger than those of the inner region; cells of the middle region were separated by many intercellular spaces (fig. 4). The outer region was composed of a single layer of epidermal-type cells. These were smaller than those of the inner region, were flattened, and contained no intercellular spaces (fig. 5). Of the three regions, the cells of the middle region comprised the majority of the megagametophyte tissue. It was in this region of the megagametophyte that the majority of protein vacuoles were found.

Megagametophyte cells from mature and stratified seeds contained irregularly shaped nuclei and angular protein vacuoles of various sizes (figs. 3–5). Globoids were present in some of the protein vacuoles (figs. 3, 4).

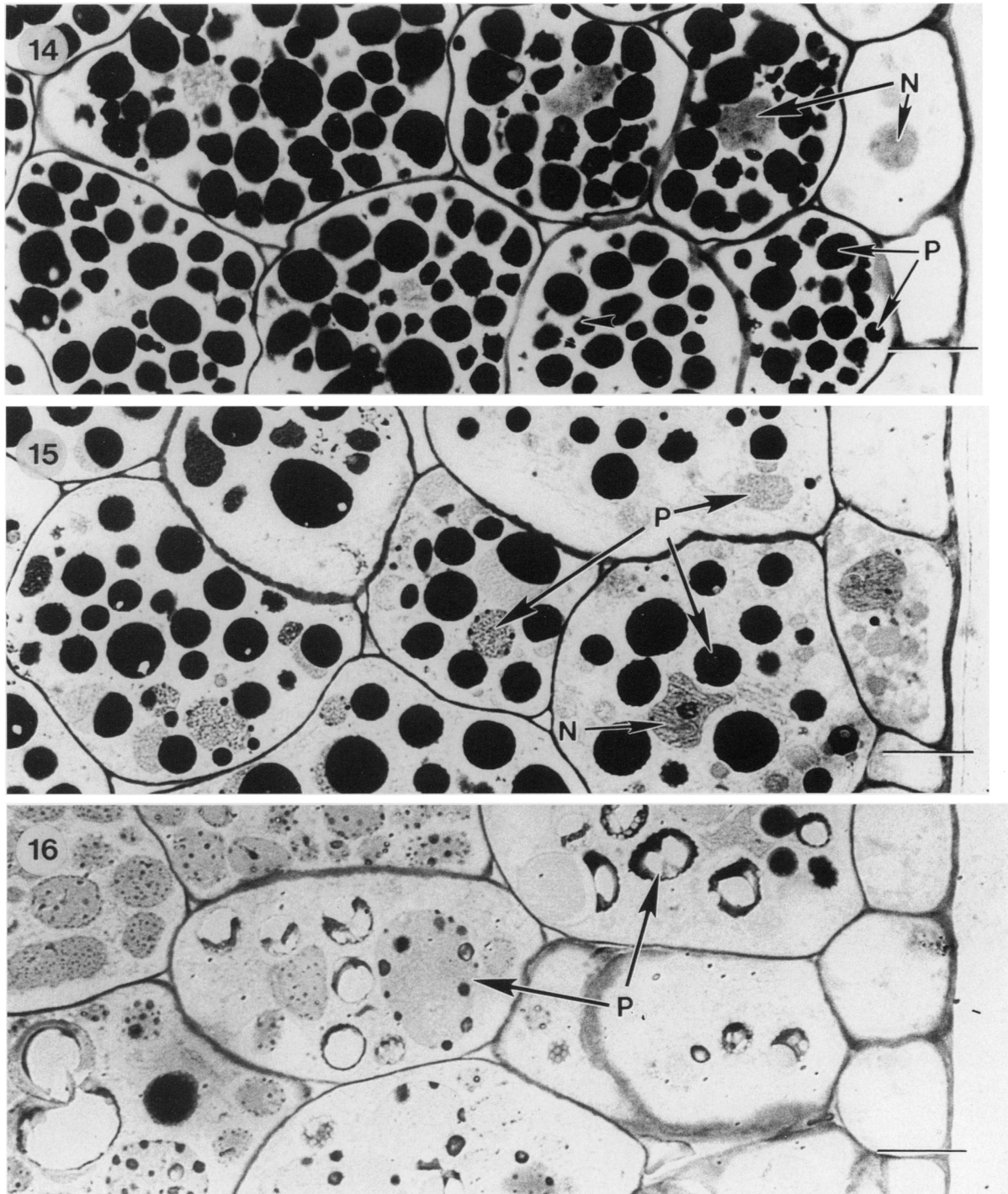
During germination, nuclei became smooth in shape and often took on an amoeboid appearance. Nucleoli were often observed. Apart from changes in nuclei, the appearance of the megagametophyte cells remained the same until germination was completed at 4 DAI₃₀.

Changes in the appearance of the inner-region megagametophyte cells were noted at 5 DAI₃₀, when the inner megagametophyte cells approximate to the carbohydrate-layer began to swell and the number of protein vacuoles in these cells declined (fig. 6). By 6 DAI₃₀, some of the innermost megagametophyte cells contained no visible protein vacuoles, whereas others contained only a few (fig. 7). The inner megagametophyte region was basically devoid of protein vacuoles by 10 DAI₃₀ (fig. 8), and large protein vacuoles, empty of protein, were clearly seen against a darkening cytoplasm by 12 DAI₃₀ (fig. 9). The cells of the middle region of the megagametophyte did not change in appearance until at least 6 DAI₃₀ (fig. 10). However, by 9 DAI₃₀ changes had occurred (fig. 11). Protein vacuoles were less numerous, less angular, and more heterogeneous in appearance. By 11 DAI₃₀ (fig. 12), protein vacuole appearance was very variable, and by 12 DAI₃₀ the number of protein vacuoles per cell fell dramatically (fig. 13). Cells close to the inner region contained only a few protein vacuoles, which had little or no protein. In contrast, protein-containing vacuoles were more numerous in cells closer to the outer region of the megagametophyte. The first change in the appearance of the megagametophyte outer region occurred at 6 DAI₃₀ (fig. 14). By then, protein vacuoles were difficult to observe. The loss of protein from protein vacuoles continued through 9 DAI₃₀ (fig. 15), and by 12 DAI₃₀ proteins in the outer-region protein vacuoles were not observed (fig. 16).

All cells of the cotyledon and hypocotyl regions of the mature or stratified seed embryo contained protein vacuoles (figs. 17, 18, and 21). However, the change in appearance of these protein vacuoles within these regions varied following imbibition at 30°C. In the procambial ring and in the developing epidermis of the hypocotyl, the protein vacuoles were depleted of protein by 4 DAI₃₀ (fig. 19). By 5 DAI₃₀, the protein vacuoles of the developing pith and cortex of the hypocotyl were depleted of protein (fig. 20). In the cotyledons, protein vacuoles of the procambial ring and epidermis were depleted of protein by 4 DAI₃₀ (fig. 22). In contrast, a decrease in protein content of protein vacuoles of the developing mesophyll was not noticeable until 5 DAI₃₀ (fig. 23). By 6 DAI₃₀, most of the protein had disappeared from the protein vacuoles in this region of the cotyledons (fig. 24).

QUANTITATIVE CHANGES IN MEGAGAMETOPHYTE AND EMBRYO OR SEEDLING PROTEINS

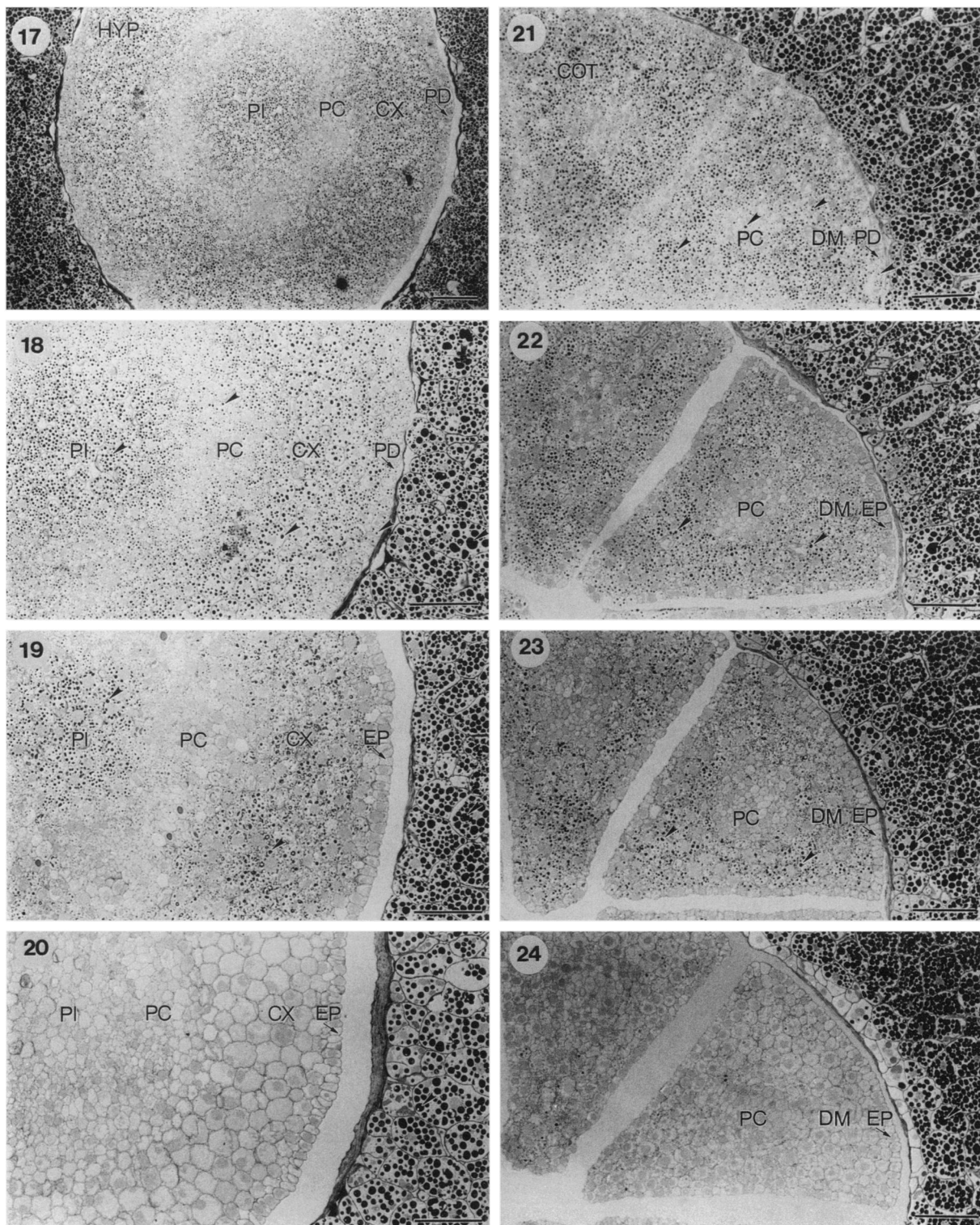
A typical mature loblolly pine seed contained 2.1 mg of protein in total, 1.9 mg in the megagametophyte, and the remaining 0.2 mg of protein in the embryo. Expressed as a percentage of seed part dry weight, the megagametophyte and embryo protein content was 19.6% and 13.1%, respectively. In the megagameto-



Figs. 14–16 Light micrographs of transverse sections through the megagametophyte showing the single cell layer of the outer region, and part of the middle region, during imbibition at 30°C. Nucleus (*N*) and protein vacuole (*P*) are shown. Bars = 20 μm . Fig. 14, 6 DAI₃₀. Outer-region protein vacuoles are undergoing protein depletion. No change in middle region protein vacuoles is evident. Fig. 15, 9 DAI₃₀. Protein vacuoles are larger and variable in appearance in the middle-region cells close to the outer region. Fig. 16, 12 DAI₃₀. Middle-region cells contain very large protein vacuoles with very little protein.

phyte, 79% of the protein was buffer insoluble. In contrast, only 27% of the embryo protein was buffer insoluble. The buffer-insoluble protein of the embryo was distributed equally between the root and shoot pole regions.

In the megagametophyte, the quantitative amount of buffer-insoluble proteins remained relatively constant throughout stratification and germination (fig. 25A). After germination was completed, the quantity of buffer-insoluble proteins began to decrease. By 12 DAI₃₀,



Figs. 17–24 Figs. 17–20, Light micrographs of transverse sections through plastic-embedded hypocotyl (*HYP*) with surrounding megagametophyte during imbibition at 30°C. Developing epidermis (*EP*), developing cortex (*CX*), procambium (*PC*), developing pith (*PI*), and protein vacuole (arrowhead) are shown. Bars = 100 μ m. Fig. 17, 35 DAI₂ stratified hypocotyl. Developing pith and cortex cells are relatively large and contain several protein vacuoles. Cells of the procambial ring and protoderm (*PD*) are relatively small and contain fewer small protein vacuoles. Fig. 18, Enlarged portion of fig. 17. Protein vacuoles appear in all cells of the 35 DAI₂ stratified hypocotyl. Fig. 19, 4 DAI₃₀. Protein vacuoles are undergoing protein loss in the developing cortex and have disappeared from the developing epidermis and procambial ring. Fig. 20, 5 DAI₃₀. Protein vacuoles are no longer visible in the hypocotyl, and imprints of hypocotyl epidermal cells in the carbohydrate layer are shown. Figs. 21–24, Light micrographs of transverse sections through plastic-embedded cotyledons (*COT*) and surrounding megagametophyte during imbibition at 30°C. Developing epidermis (*EP*), procambium (*PC*), developing mesophyll (*DM*), and protein vacuole (arrowhead) are shown. Bars = 100 μ m. Fig. 21, Protein vacuoles are present in all the cells of 35 DAI₂ stratified cotyledons. Developing mesophyll cells are large and contain the largest protein vacuoles of the cotyledons. Protodermal (*PD*) and procambial cells

buffer-insoluble protein levels were only 10% of those found in mature seed megagametophytes. In contrast, the megagametophyte buffer-soluble protein pool increased following the completion of germination, reaching maximum levels by 10 DAI₃₀.

The buffer-insoluble protein levels in the shoot and root pole regions of the embryo or seedling remained constant until 2 DAI₃₀, after which a decrease was observed in both regions (fig. 25B). In the root pole, the level of buffer-insoluble protein decreased to a minimum at 3 DAI₃₀, while the shoot pole level reached a minimum at 4 DAI₃₀. Buffer-insoluble protein levels then increased in both poles; the increase in the root pole region was greater. The levels of buffer-soluble protein in the shoot and root pole regions were also relatively constant during germination and the initial stages of early-seedling growth (fig. 25B). By 6 DAI₃₀, increases in both protein pools were seen. However, by 12 DAI₃₀, the buffer-soluble protein content of the shoot pole region was significantly higher than that of the root pole region of the seedling. At this stage of seedling development, the average buffer-soluble protein content was 1.2 mg per seedling, of which 78% was in the shoot pole region.

SDS-dissociated extracts of shoot and root pole regions from mature seed embryos contained three major buffer-insoluble proteins; molecular masses of 47, 37.5, and 22.5 kD (lane *M* in fig. 26A, B). Breakdown of these proteins was less rapid in the shoot pole region. The depletion of the shoot pole 47-kD protein band began at 4 DAI₃₀ and was complete by 8 DAI₃₀ (fig. 26A). In contrast, the depletion of the equivalent root pole protein band began at 3 DAI₃₀ and was complete by 4 DAI₃₀ (fig. 26B). The start of breakdown of the 37.5- and 22.5-kD protein bands were similar in both the root and shoot poles of the embryo, 4 DAI₃₀ (fig. 26A, B), but the rates of breakdown were different. In the shoot pole, these proteins, although significantly depleted, were still present by 11 DAI₃₀ (fig. 26A), whereas the 37.5- and 22.5-kD polypeptide bands of the root pole were depleted by 7 DAI₃₀ (fig. 26B).

Discussion

During 35 d of stratification at 2°C, the relative water content of loblolly pine seeds increased from 6% to 23% (Schneider and Gifford 1994). Despite this increase, there was virtually no change in the appearance of mature and fully stratified cells of either the megagametophyte or the embryo, nor were there changes in the amounts of buffer-soluble or -insoluble proteins. The large change in relative water content during this time likely had little effect on the appearance of the cells, because of the abundance of storage reserves. However, the appearance of the carbohydrate-positive

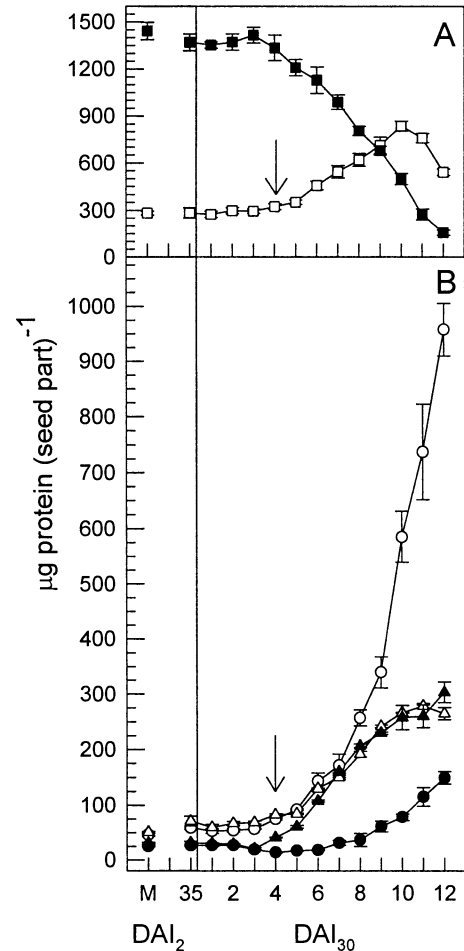


Fig. 25 Quantitative changes in buffer-soluble and -insoluble proteins of the megagametophyte (A) and embryo or seedling (B) following imbibition at 30°C. X-axis shows mature seed (*M*), stratified seed (35 DAI₂), and seed imbibed for up to 12 DAI₃₀. Arrows show time of completion of germination, as indicated by radicle emergence from the seed coat. Megagametophyte buffer-soluble (open squares) and buffer-insoluble protein (solid squares), embryo or seedling shoot pole buffer-soluble (open circles) and -insoluble protein (solid circles), and embryo or seedling root pole buffer-soluble (open triangles) and -insoluble (solid triangle) protein are shown. Each data point is the mean of three determinations \pm SE.

layer did change with stratification from thin, dry, and flaky to moist and malleable. As this hydration occurred, there was a slight decrease in the size of the corrosion cavity. It is interesting that the corrosion cavity was never fluid filled. When the seedling was dissected from the seed, the surfaces in contact with the corrosion cavity were moist, but no extra liquid was present. Throughout stratification, germination, and early-seedling growth, the megagametophyte and the embryo or seedling maintained a close physical

←

contain fewer and smaller protein vacuoles. Fig. 22, 4 DAI₃₀. Protein vacuoles in the developing epidermis and procambium are undergoing some protein loss. Fig. 23, 5 DAI₃₀. Protein vacuoles are no longer visible in most of the developing epidermis and procambium. Protein depletion is occurring in the developing mesophyll. Fig. 24, 6 DAI₃₀. Protein vacuoles are no longer visible in most of the cotyledon cells.

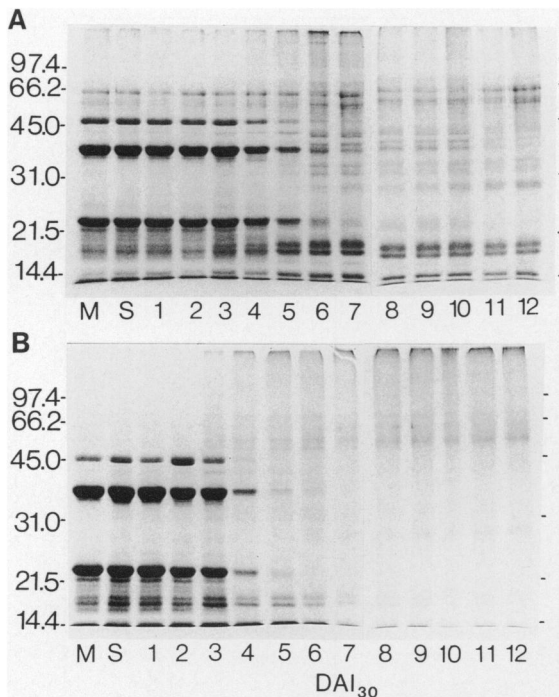


Fig. 26 Coomassie blue-stained SDS-PAGE profile of buffer-insoluble proteins from embryo or seedling shoot and root poles following imbibition, run under reducing conditions in the presence of 2-mercaptoethanol. *A*, shoot poles; *B*, root poles. For each lane, 3 μ g protein was loaded in 10 μ L. Relative molecular masses of standards (in kD) are shown by numerical values adjacent to the gel profiles. Lanes are mature seed (*M*), 35 DAI₂ stratified seed (*S*), and seed imbibed for up to 12 DAI₃₀.

relationship. Evidence for this could be seen in the carbohydrate-positive layer. As the cotyledons expanded and grew during germination and early-seedling growth, they pressed against the layer, leaving clear imprints of their epidermal cells. The hypocotyl was also in close contact with the carbohydrate-positive layer, while still inside the megagametophyte and imprints of its epidermal cells were also seen.

In conifers and many dicotyledons, protein vacuoles are formed during seed development by the deposition of storage proteins into fragmenting (Craig et al. 1980; Collada et al. 1993; Owens et al. 1993) or fragmented (Gifford et al. 1982) vacuoles. At maturity and after stratification, protein vacuoles of loblolly pine megagametophyte and embryo cells were uniformly dense and angular. Each protein vacuole usually contained a globoid, as has been observed for several other conifers (Simola 1974b; Misra and Green 1990; Green et al. 1991). The protein vacuoles were of various sizes in any given cell. In general, loblolly pine protein vacuoles were much larger in megagametophyte cells than in embryo cells, as has been observed for protein vacuoles of *Picea glauca* (Krasowski and Owens 1993) and *Pseudotsuga menziesii* (Owens et al. 1993).

During germination and early-seedling growth, loblolly pine protein vacuoles underwent changes in appearance related to storage protein hydrolysis. Soon

after storage protein hydrolysis began, the protein vacuoles became more rounded. Protein vacuoles then coalesced, forming larger proteinaceous vacuoles. Protein vacuole fusion was more noticeable in megagametophyte cells than in seedling cells.

In loblolly pine the major storage proteins were a 47-kD globulin and a glutelin-like crystalloid protein (Groome et al. 1991); both were buffer insoluble. The crystalloid protein consisted of six subunits, and each subunit was composed of two disulphide-bridged polypeptides of molecular mass 37.5 and 22.5 kD (Groome et al. 1991). These protein reserves were found in both the seedling and megagametophyte. They were depleted more rapidly in the seedling, as has been observed for other conifers (Simola 1974a, 1974b, 1976; Cardemil and Reiner 1982; De Carli et al. 1987). Within the seedling, the protein reserves were depleted more rapidly in the root pole, as has been observed for *Picea excelsa* (De Carli et al. 1987) and *Picea abies* (Simola 1976). The more rapid mobilization of protein reserves in loblolly pine root poles was likely due to a high demand for energy and amino acid building blocks in this tissue during germination as radicle expansion was occurring (De Carli et al. 1987).

An interesting pattern of protein vacuole change was found in the megagametophyte, where it occurred in two separate directional waves. The first and major wave began in the inner layer of megagametophyte cells at 5 DAI₃₀ and then progressed into the middle region of the megagametophyte. The second, minor, wave began at 6 DAI₃₀ in the outer layer and then progressed into the middle region of the megagametophyte. This wave moved slower than the first. Corresponding with these waves was a decrease in megagametophyte buffer-insoluble protein content, which started at 5 DAI₃₀ and became rapid after 8 DAI₃₀. The result of the two waves could be clearly seen by 12 DAI₃₀ when the majority of the protein-containing protein vacuoles were observed in the outer half of the megagametophyte middle region. The reason for this hydrolysis pattern is unknown at present. A gradient in protein body vacuolation was observed for *P. excelsa* seeds during germination and early-seedling growth (De Carli et al. 1987) in which protein vacuoles of the inner megagametophyte region were vacuolated before those of the middle region. No observations, however, were presented to indicate the presence or absence of a second protein body gradient from the outer region toward the middle region of the megagametophyte.

Acknowledgments

Funding for this research was provided to David J. Gifford by the Natural Sciences and Engineering Research Council of Canada (NSERC) (operating grant OGP0002240) and to Sandra L. Stone with NSERC postgraduate scholarships A and B. Special thanks to Dr. D. D. Cass for his advice and the use of his sectioning equipment and photomicroscope.

Literature cited

- Burk RR, M Eschenbruch, P Leuthard, G Steck 1983 Sensitive detection of proteins and peptides in polyacrylamide gels after formaldehyde fixation. *Methods Enzymol* 91:247–254.
- Burrows GE, RA Stockey 1994 The developmental anatomy of cryptogal germination in bunya pine (*Araucaria bidwillii*). *Int J Plant Sci* 155:519–537.
- Cardemil L, A Reinero 1982 Changes of *Araucaria araucana* seed reserves during germination and early seedling growth. *Can J Bot* 60:1629–1638.
- Ching TM 1966 Compositional changes of Douglas fir seeds during germination. *Plant Physiol* 41:1313–1319.
- Collada C, I Allona, P Aragoncillo, C Aragoncillo 1993 Development of protein bodies in cotyledons of *Fagus sylvatica*. *Physiol Plant* 89:354–359.
- Craig S, A Millerd, DJ Goodchild 1980 Structural aspects of protein accumulation in developing pea cotyledons. III. Immunocytochemical localization of legumin and vicilin using antibodies shown to be specific by the enzyme-linked immunosorbent assay (ELISA). *Aust J Plant Physiol* 7:339–351.
- De Carli ME, B Balden, P Mariani, N Rascio 1987 Subcellular and physiological changes in *Picea excelsa* seeds during germination. *Cytobios* 50:29–39.
- Durzan DJ, V Chalupa 1968 Free sugars, amino acids, and soluble proteins in the embryo and female gametophyte of jack pine as related to climate at the seed source. *Can J Bot* 46:417–428.
- Durzan DJ, AJ Mia, PK Ramaiah 1971 The metabolism and subcellular organization of the jack pine embryo (*Pinus banksiana*) during germination. *Can J Bot* 49:927–938.
- Gifford DJ 1988 An electrophoretic analysis of the seed proteins from *Pinus monticola* and eight other species of pine. *Can J Bot* 66:1808–1812.
- Gifford DJ, JS Greenwood, JD Bewley 1982 Deposition of matrix and crystalloid storage proteins during protein body development in the endosperm of *Ricinus communis* L. cv. Hale seeds. *Plant Physiol* 69:1471–1478.
- Gifford EM 1950 Softening refractory plant material embedded in paraffin. *Stain Technol* 25:161–162.
- Gori P 1979 An ultrastructural investigation of protein and lipid reserves in the endosperm of *Pinus pinea* L. *Ann Bot* 43:101–105.
- Green MJ, JK McLeod, S Misra 1991 Characterization of Douglas fir protein body composition by SDS-PAGE and electron microscopy. *Plant Physiol Biochem* 29:49–55.
- Groome MC, SR Axler, DJ Gifford 1991 Hydrolysis of lipid and protein reserves in loblolly pine seeds in relation to protein electrophoretic patterns following imbibition. *Physiol Plant* 83:99–106.
- Hammer MF, JB Murphy 1994 Lipase activity and *in vivo* triacylglycerol utilization during *Pinus edulis* seed germination. *Plant Physiol Biochem* 32:861–867.
- Hoff RJ 1987 Dormancy in *Pinus monticola* seed related to stratification time, seed coat and genetics. *Can J For Res* 17:294–298.
- Jensen WA 1962 Botanical histochemistry: principles and practice. W. H. Freeman, San Francisco.
- King JE, DJ Gifford 1997 Amino acid utilization in seeds of loblolly pine during germination and early seedling growth. I. Arginine and arginase activity. *Plant Physiol* 113:1125–1135.
- Kovac M, I Kregar 1989 Starch metabolism in silver fir seeds during germination. *Plant Physiol Biochem* 27:873–880.
- Krasowski MJ, JN Owens 1993 Ultrastructural and histochemical postfertilization megagametophyte and zygotic embryo development of white spruce (*Picea glauca*) emphasizing the deposition of seed storage products. *Can J Bot* 71:98–112.
- Laemmli UK 1970 Cleavage of structural proteins during the assembly of the head of bacteriophage T4. *Nature* 227:680–685.
- Lammer DL, DJ Gifford 1989 Lodgepole pine seed germination. II. The seed proteins and their mobilization in the megagametophyte and embryonic axis. *Can J Bot* 67:2544–2551.
- Lowry OH, NJ Rosebrough, AL Farr, RJ Randall 1951 Protein measurement with the Folin phenol reagent. *J Biol Chem* 193:265–275.
- Misra S 1994 Conifer zygotic embryogenesis, somatic embryogenesis, and seed germination: biochemical and molecular advances. *Seed Sci Res* 4:357–384.
- Misra S, MJ Green 1990 Developmental gene expression in conifer embryogenesis and germination. I. Seed proteins and protein body composition of mature embryo and the megagametophyte of white spruce (*Picea glauca* [Moench] Voss.). *Plant Sci* 68:163–173.
- Mullen RT, DJ Gifford 1995 Purification and characterization of the glyoxysomal enzyme malate synthase following seed germination in *Pinus taeda*. *Plant Physiol Biochem* 33:639–648.
- Mullen RT, JE King, DJ Gifford 1996 Changes in mRNA populations during loblolly pine (*Pinus taeda*) seed stratification, germination and post-germinative growth. *Physiol Plant* 97:545–553.
- Murphy JB, MF Hammer 1988 Respiration and soluble sugar metabolism in sugar pine embryos. *Physiol Plant* 74:95–100.
- 1994 Starch synthesis and localization in post-germination *Pinus edulis* seedlings. *Can J For Res* 24:1457–1463.
- O'Brien TP, ME McCully 1981 The study of plant structure: principles and selected methods. Termarcarphi, Melbourne.
- Owens JN, SJ Morris, S Misra 1993 The ultrastructural, histochemical, and biochemical development of the post-fertilization megagametophyte and the zygotic embryo of *Pseudotsuga menziesii*. *Can J For Res* 23:816–827.
- Salmia MA 1981 Fractionation of the proteinases present in the endosperm of germinating seed of Scots pine, *Pinus sylvestris*. *Physiol Plant* 51:253–258.
- Sasaki S, TT Kozlowski 1969 Utilization of seed reserves and currently produced photosynthates by embryonic tissues of pine seedlings. *Ann Bot* 33:473–482.
- Schneider W, DJ Gifford 1994 Loblolly pine seed dormancy. I. The relationship between protein synthesis and the loss of dormancy. *Physiol Plant* 90:246–252.
- Simola LK 1974a Subcellular organization of cotyledons of *Picea abies* during germination. *Port Acta Biol* 14:413–428.
- 1974b Ultrastructure of dry and germinating seeds of *Pinus sylvestris* L. *Acta Bot Fenn* 103:1–31.
- 1976 Changes in the subcellular organization of endosperm and radicle cells of *Picea abies* during germination. *Z Pflanzenphysiol Bd* 78(suppl):41–51.
- Singh H, BM Johri 1972 Development of gymnosperm seeds. Pages 21–75 in TT Kozlowski, ed. *Seed biology*. Vol 1. Academic Press, New York.
- Spurr AR 1969 A low-viscosity epoxy resin embedding medium for electron microscopy. *J Ultrastruct Res* 26:31–43.